

Disponible en www.hormigonyacero.com
Hormigón y Acero, 2023
<https://doi.org/10.33586/hya.2023.3130>

ARTÍCULO EN AVANCE ON LINE

Energy Flow Considerations for Structural Response under Blast

K. Willems, T. Krauthammer, & A. Ohrt
DOI: <https://doi.org/10.33586/hya.2023.3130>

Para ser publicado en: *Hormigón y Acero*

Por favor, el presente artículo debe ser citado así:

Willems, K., Krauthammer, T., & Ohrt, A. (2023) Energy Flow Considerations for Structural Response under Blast, *Hormigón y Acero*, <https://doi.org/10.33586/hya.2023.3130>

Este es un archivo PDF de un artículo que ha sido objeto de mejoras propuestas por dos revisores después de la aceptación, como la adición de esta página de portada y metadatos, y el formato para su legibilidad, pero todavía no es la versión definitiva del artículo. Esta versión será sometida a un trabajo editorial adicional, y una revisión más antes de ser publicado en su formato final, pero presentamos esta versión para adelantar su disponibilidad.

En el proceso editorial y de producción posterior pueden producirse pequeñas modificaciones en su contenido.

© 2023 Publicado por CINTER Divulgación Técnica para la Asociación Española de Ingeniería Estructural, ACHE

Energy Flow Considerations for Structural Response under Blast

K. Willems, T. Krauthammer

Center for Infrastructure Protection and Physical Security (CIPPS), University of Florida

A. Ohrt

Air Force Research Laboratory (AFRL/RWML), Eglin AFB, FL

ABSTRACT

Load-impulse (P-I) diagrams are commonly used for structural design and damage assessment. Recently, an energy-based alternative to P-I diagrams, known as Energy vs. Energy Rate (E-R) diagrams, was proposed. E-R diagrams are another tool for structural design and damage assessment from an energy flow perspective. This paper describes a study to assess and compare these two analytical approaches, and to provide examples for illustrating the findings.

INTRODUCTION

A load-impulse (P-I) diagram is a well-accepted tool that is commonly used to aid structural engineers for structural strength design, as well as for potential damage assessment. Recently, an energy-based alternative to P-I diagrams, known as Energy vs. Energy Rate (E-R) diagrams, was proposed. Two simple conversion equations were also proposed to transform P-I data into E-R data. The E-R diagram serves as another tool for a structural engineer to use and gives the ability to analyze a structural element from an energy-based perspective. This research provides [1] an in-depth check of the validity of the E-R diagram by comparing the energy approach to generally accepted forms of structural analysis. The analytical solutions for rectangular and triangular loads that were previously proposed were checked against results from a validated a single-degree-of-freedom. The energy flow-based approach was used to analyze several structural elements under severe dynamic loads.

BACKGROUND

Structural behavior can be characterized over a wide frequency range from the quasi-static to impulsive, as described in Table 1 [2], and illustrated in Figure 1 [3-5]. These behaviors are based on the response of a single-degree-of-freedom (SDOF) system that has the following equation of motion [2]:

$$M\ddot{x} + C\dot{x} + Kx = F(t) \quad (1)$$

In which, M is the mass, C is the damping coefficient, K is the stiffness, and F(t) is the forcing function. Dividing Eq. (1) by the mass, M, results in the following equation:

$$\ddot{x} + \frac{C}{M}\dot{x} + \frac{K}{M}x = \frac{F}{M}(t) \quad (2)$$

Eq. (2) can be rewritten, as follows:

$$\ddot{x} + 2\xi\omega\dot{x} + \omega^2x = f(t) \quad (3)$$

Where:

$$\omega = \sqrt{K/M} \quad (4a)$$

$$\omega = \omega\sqrt{1 - \xi^2} \quad (4b)$$

$$\xi = C/C_{cr} \quad (4c)$$

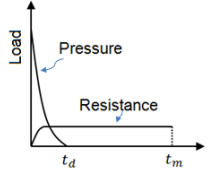
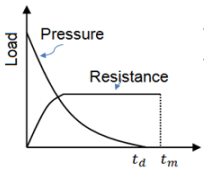
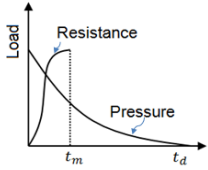
$$C_{cr} = 2\sqrt{KM} \quad (4d)$$

In Equations (4a – 4d), ω is the circular natural frequency that equals $2\pi f$; f is the natural frequency that is equal to $1/T$, where T is the natural period. ξ is the damping ratio, and C_{cr} is the value of critical damping. ω is the damped circular natural frequency. \ddot{x} , \dot{x} , and x are the acceleration, velocity, and displacement of the mass, respectively. Also, the term $(K/M)x$ in Eq. (2) can be replaced by a resistance function, $R(x)$ that represents a nonlinear relationship between load and deflection. A structural element can be represented by a SDOF equation (Eq.

1), but the parameters for mass, stiffness and force must be replaced by their equivalent values for the continuous structural element, as discussed in [2]. Solving Eq. (3), either numerically or in closed form, will provide the time histories for the structural motions.

The theoretical concept of load-impulse (P-I) diagrams is based on the definition of a response spectrum that has been known for several decades [6, 7]. P is either load or pressure, depending on how the loading function is defined for a specific problem. The impulse, I, is defined as the area under the load-time or pressure-time histories. It is known that a P-I diagram has two theoretical asymptotes: An impulsive asymptote that is derived by assuming that the amount of input kinetic energy is equal to the resulting internal strain energy, and a quasi-static asymptote that is derived by assuming that the amount of input external work is equal to the resulting internal strain energy. The structural assessment is done by plotting the load point (i.e., defined by the values of peak pulse pressure and the impulse, which is the area under the pulse) on the P-I diagram. Failure is defined if the point falls on or above the P-I curve. Unfortunately, the P-I diagram cannot be derived only from such energy-based principles. Therefore, the theoretical approach had serious limitations that prevented one from applying it for the analysis of physical structures [7]. The development of a physics-based fast-running numerical approach for deriving P-I diagrams has created the ability to assess the behavior of structural elements under realistic loads [8], and the approach enabled one to derive complete P-I diagrams for different structural elements (e.g., beams, slabs, columns, etc.) and different structural response mechanisms (flexure with or without diagonal shear effects, direct shear, etc.).

Table 1. Load and structural behavior domains [2,3,6]

Illustrations			
Loading range	Impulsive	Dynamic	Quasi-Static
Pressure range	High	Intermediate	Low
Load duration	Short	Intermediate	Long
Response time	Long	Intermediate	Short
$\frac{t_m}{t_d}$	$\frac{t_m}{t_d} > 3$	$3 > \frac{t_m}{t_d} > 0.1$	$\frac{t_m}{t_d} < 0.1$
Approximate limits	$\frac{t_d}{T} < 0.0637$	$0.0637 < \frac{t_d}{T} < 6.37$	$\frac{t_d}{T} > 6.37$

Where, T is the natural period, t_d is the duration of the applied load, and t_m is the time at which the maximum structural response is reached.

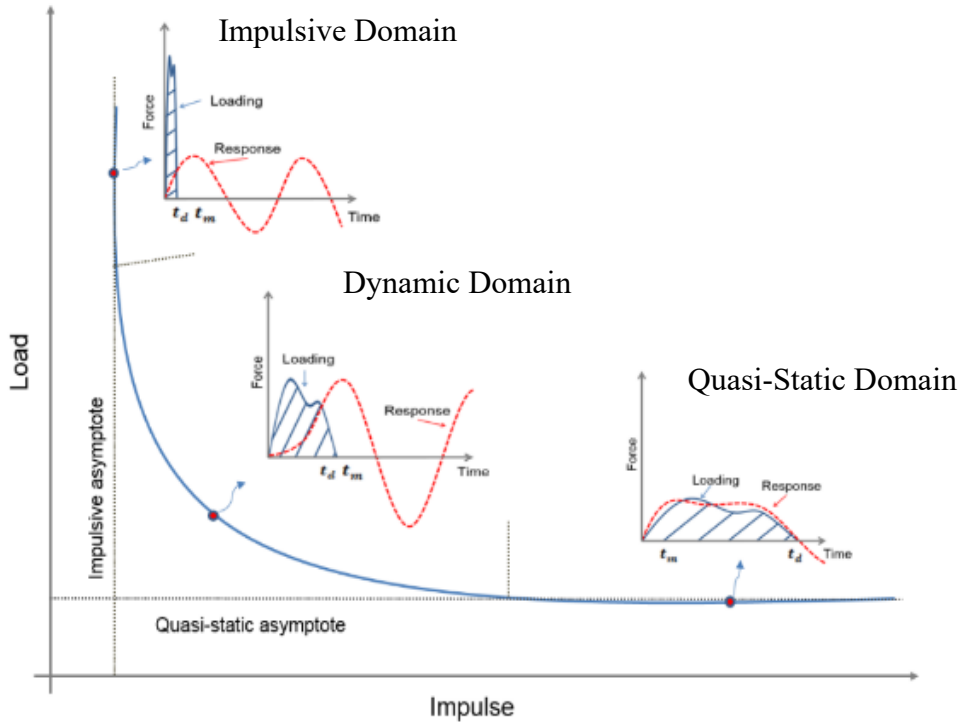


Figure 1. P-I diagram and load pulse domains [3]

A further development in [3-5] explored how to address the relationships between the applied load and the structural response by using energy flow principles. Also, the same effort identified and characterized the energy-based relationships with the concept of P-I curves. It was shown in [3-5] that the maximum strain energy can be used to find the maximum values of kinetic, KE_{max} , and work WE_{max} , energies, and the time when they are reached, t_m , as shown in Table 2.

Table 2. Max Energy Functions for undamped SDOF under Rectangular Loads [3-5]

Response domain		Forced vibration			Free vibration		
Term		t_m	Range	Max	t_m	Range	Max
Maximum kinetic energy	KE_{max}	$\frac{\pi}{2\omega}$	$\omega t_d \geq \frac{\pi}{2}$	$\frac{F_o^2}{2k}$	$\frac{2\pi + \omega t_d}{2\omega}$	$0 \leq \omega t_d < \frac{\pi}{2}$	$\frac{2F_o^2}{k} \sin\left(\frac{\omega t_d}{2}\right)^2$
Maximum strain energy	SE_{max}	$\frac{\pi}{\omega}$	$\omega t_d \geq \pi$	$\frac{2F_o^2}{k}$	$\frac{\pi + \omega t_d}{2\omega}$	$0 \leq \omega t_d < \pi$	$\frac{2F_o^2}{k} \sin\left(\frac{\omega t_d}{2}\right)^2$
Maximum external energy	WE_{max}	$\frac{\pi}{\omega}$	$\omega t_d \geq \pi$	$\frac{2F_o^2}{k}$	$t_m = t_d$	$0 \leq \omega t_d < \pi$	$\frac{2F_o^2}{k} \sin\left(\frac{\omega t_d}{2}\right)^2$

Where, F_0 is the peak load, t_d is the load duration, ω is the circular natural frequency from classical structural dynamics [2] (see Eq. 4a, above), f is the natural frequency, k is the spring stiffness in the SDOF system, and t_m is the time when maximum value is reached. Also, there is no work done by external load after the load has been removed from the system. The maximum value occurs at $t = t_d$ for a rectangular load pulse. An energy component spectrum can be plotted by collecting each of the three energy components at $t = t_d$. Figure 2 shows the energy transition at the end of the loading durations, based on the ratio of t_d/T . Each of the energy terms, work energy (WE), strain energy (SE), and kinetic energy (KE), are all normalized by a ratio of the peak load (F_0) squared to the elastic spring stiffness (k). A general energy-based solution to

define the entire domain of a P-I diagram was proposed in [3-5], and it illustrated for a simplified system with a simplified load profile in Table 3 for an elastic SDOF system.

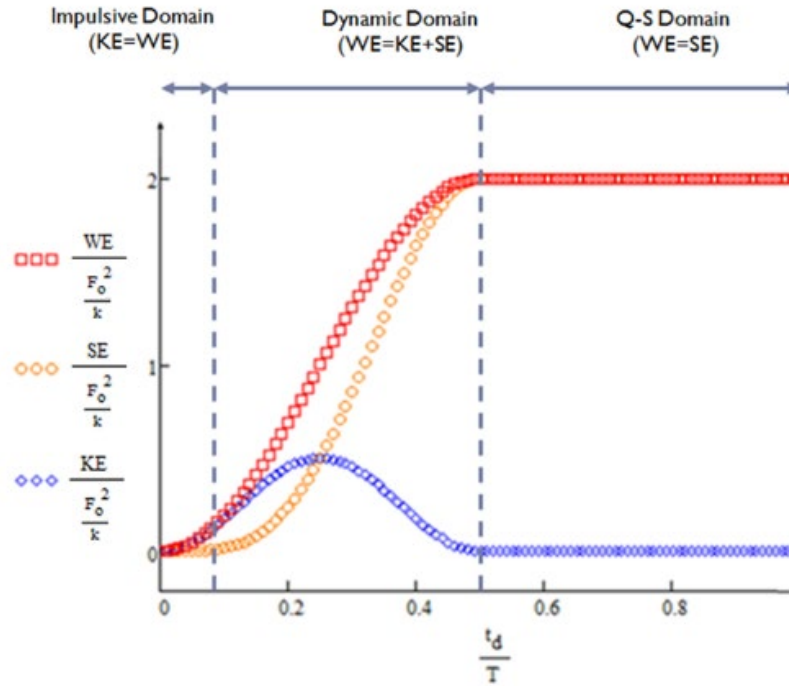


Figure 2. Typical energy components spectra [3].

Table 3. Summary of Energy Based Solutions for P-I Diagrams [3-5].

Load-response illustration			
Loading regime	Impulsive	Dynamic	Quasi-Static
Load duration	Short	Medium	Long
Response time	Long	Medium	Short
$t = t_d$	$WE_{t_d} = KE_{t_d}$	$WE_{t_d} = KE_{t_d} + SE_{t_d}$	$WE_{t_d} = KE_{t_d} + SE_{t_d}$
$t = t_m$	$WE_{t_m} = SE_{t_m}$	$WE_{t_m} = SE_{t_m}$	$WE_{t_m} = SE_{t_m}$
Absorbed energy	$KE_{t_d} = \frac{I^2}{2M}$	$WE_{t_d} = \frac{1}{2}Mv_{t_d}^2 + \frac{1}{2}ku_{t_d}^2$	$WE_{t_m} = F_0u_{max}$
Asymptotes	$KE_{t_d} = SE_{t_m}$	$KE_{t_d} + SE_{t_d} = SE_{t_m}$	$WE_{t_m} = SE_{t_m}$

Where, u_{max} is the maximum displacement, I is the impulse, and M is the mass.

Load Pulse Shape Factor (Beta), and its relationship with scaled distance

As noted above, the relationship between the peak load, duration, and impulse can be described as the load pulse shape factor, β . For a simplified load pulse, the area under the normalized load vs. time plot is the load pulse shape factor. The normalized load vs. time plot can be obtained by dividing all the time values by the load duration, t_d , and all the load values by the peak load, F_0 . For a rectangular load pulse, the load pulse shape factor is: $\beta = 1$. For a triangular load pulse, the load pulse shape factor is: $\beta = 1/2$. For an exponentially decaying load pulse, such as a simplified blast load pulse, there are a range of load pulse shape factors that are all smaller than $\beta = 1/2$. The influence of the Beta value on P-I and E-R diagrams will be studied and preliminary results of this study will be addressed later, herein. The scaled distance, Z , for a blast load is calculated by dividing the standoff distance, R , by the cubed root of the TNT charge weight, W , as shown in Equation (5).

$$Z = \frac{R}{W^{\frac{1}{3}}} \quad (5)$$

The concept of Z , as discussed in [7,11], is that incidents with the same value of Z will exhibit virtually identical consequences. For a given scaled distance, blast load characteristics such as peak pressure, scaled impulse, and scaled duration can be read from a single chart. The scaled distance, Z , is an important concept since one can use specific values of Z for structural analyses, instead of specifying values of charge weights and distances. While it is not currently listed as a value on the charts in UFC 3-340-02 [10], one could calculate a new set of data points to overlay onto the UFC charts that represent a β value for each scaled distance. These data points can be calculated by dividing the scaled impulse by the peak pressure and the scaled duration, as shown in Equation (6). Since the charts have values for both incident and reflected pressures, β values can also be calculated for both incident and reflected blasts.

$$\beta = \frac{\left(\frac{I}{W^{1/3}}\right)}{P_o * \left(\frac{t_d}{W^{1/3}}\right)} \quad (6)$$

The load pulse shape factor is a unitless value. Therefore, a single β value can be used to describe many peak loads and load durations, as shown in Figure 3.

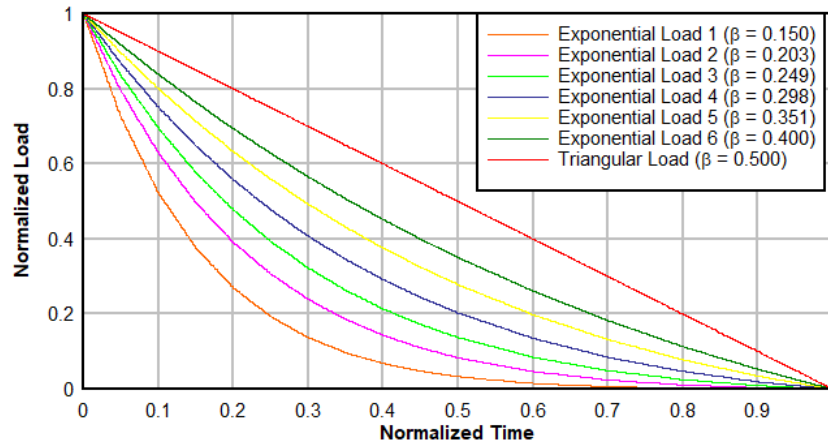


Figure 3. Beta – defined normalized load functions.

For example, a β value of 0.200 can be scaled up to describe a peak load of 100 kips and a load duration of 15 milliseconds, or a load pulse with a peak load of 50 kips and 20 milliseconds.

Since the β value is the area under the normalized load vs. time plot, the impulse delivered by the given load is given by Equation (7).

$$I_{impulse} = \beta \cdot F_o \cdot t_d \quad (7)$$

Where, $W^{1/3}$ indicates that the impulse, I , and pulse duration, t_d , were scaled by the cube root of the TNT equivalent explosive weight, as defined in [10]. Different exponential load functions that have the same Beta value will yield the exact same P-I and E-R diagrams. The influence of β on the three domains in P-I or E-R diagrams, as discussed next.

For an energy-based P-I diagram, the energy input and the input rate must be able to be defined accurately. It was shown in [3-5] that, for a structure subjected to a given load pulse with a duration (t_d), the input energy, input energy rate, and the energy imparted to the system can be defined by Equations (8–10).

$$E_{input} = \frac{(I_{impulse})^2}{2 \cdot M_{mass}} = \frac{(\beta \cdot F_o \cdot t_d)^2}{2 \cdot M_{mass}} \quad (8)$$

$$E_{input_{rate}} = \frac{E_{input}}{\beta \cdot t_d} \quad (9)$$

$$E_{imparted} = \int_0^{u_{max}} kudu \quad (10)$$

Where, E_{input} is the input energy, $E_{input_{rate}}$ is the input energy rate, $E_{imparted}$ is the energy imparted to the system (absorbed energy), $I_{impulse}$ is the impulse delivered to system (area under load-time history), M_{mass} is the mass of the system, β is the load pulse shape factor that affects the rate of decay of the load pulse, as discussed later, herein. F_o is the peak load, P_0 is the peak pressure (in case the load function is defined by a force), t_d is the load duration, and u_{max} is the maximum displacement, and/or the given response limit. The idea of an energy component spectrum was discussed previously. In the same way that the energy component spectrum was developed, an input energy spectrum can be created, with each point on the curve representing the same response limit [3-5]. The difference between the energy input to the system and the energy imparted to the system can be found by using the following equation.

$$E_{difference} = E_{input} - E_{imparted} \quad (11)$$

The energy difference spectrum is shown in Figure 4, where load pulses with shorter durations result in lower energy differences. As the energy input rate increases, less energy is needed to

reach a desired response limit. This can be seen for the case where a fixed amount of energy is applied to a system and the input energy rate is changed.

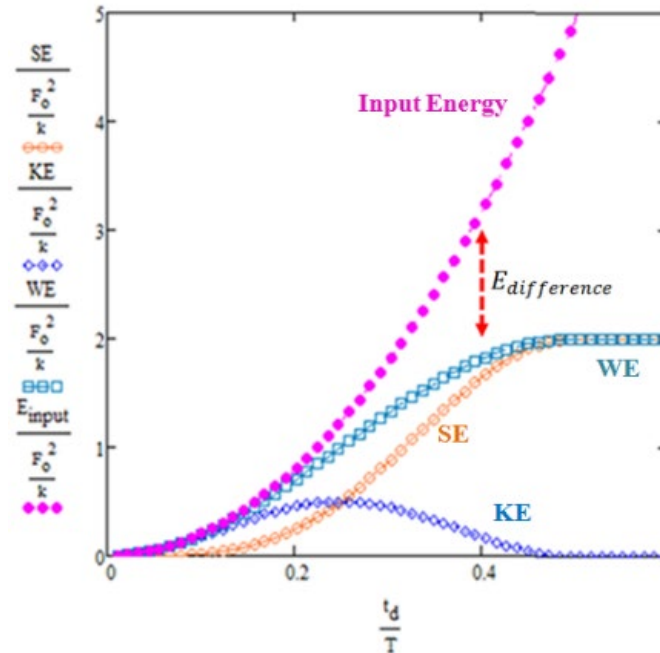


Figure 4. Energy components spectrum for a rectangular load pulse [3]

The underlying idea for the methods mentioned in this section is energy flow. The input energy, sometimes referred to as the energy input, is described as the total amount of energy that is delivered to the structural system. Some of this input energy will do work on the system, but some of it may not do work. The rate at which the input energy is delivered to the system is called the input energy rate. The input energy rate can also be referred to as the power, P , generated by the input energy. The amount of input energy that does work on the system is called the imparted energy. This type of energy is also commonly called the absorbed energy. Finally, the amount of input energy that does not do work on the system is called the energy difference. This value can be calculated by finding the difference between the input energy and the imparted energy. The amount of energy that is delivered from the energetic loads source determines how

the structure reacts. The rate at which this energy enters the structural system is also a critical factor in determining structural response. An E-R diagram (or an energy-power, E-P, diagram) allows the user to look at how much energy and at what rate it is entering the structural system to determine the structural responses. These diagrams have only been proposed in [3-5] for simplified load pulses, so there is a need to determine if the process is the same for non-simplified load pulses on realistic structures.

Energy rate vs. energy diagrams

A typical energy-based diagram (the equivalent to a P-I diagram in the energy rate vs. energy) has the horizontal axis defined as the input energy and the vertical axis as the input energy rate. These diagrams work the same way that traditional P-I diagrams do, with combinations that fall to the right and above the curve representing the limit state has been reached. E-R diagrams allow a designer to look at the response of the structure from an energy standpoint. The dimensionless terms for the energy input and energy input rate, the axes for the E-R diagram for an undamped elastic SDOF system were defined in [3-5] by the following equations.

$$\bar{E} = \frac{E_{input}}{E_{imparted}} = \frac{\frac{I^2}{2m}}{\frac{1}{2}k u_{max}^2} = \frac{I^2}{k m u_{max}^2} \quad (12)$$

$$\bar{R} = \frac{E_{input_{rate}}}{E_{imparted} \omega} = \frac{\frac{(\beta F_o t_d)^2}{2m} \frac{1}{\beta t_d}}{\frac{1}{2}k u_{max}^2 \omega} = \frac{\beta F_o^2 t_d}{k^{\frac{3}{2}} m^{\frac{1}{2}} u_{max}^2} \quad (13)$$

$$\frac{\bar{E}}{\bar{R}} = \beta \omega t_d \quad (14)$$

Equations (12-13) can be used for deriving the E-R diagrams for any type of load pulse, as shown in Figure 5 for rectangular and triangular load pulses. One note that the impulsive asymptote shown in Figure 5 is defined by Eq. (13) that is a ratio of the rate of E_{input} to

Eimparted times $\omega = 2\pi f$, as defined earlier herein. It shows that, at high loading rates and when the system is in the impulsive domain, this ratio approaches 1.

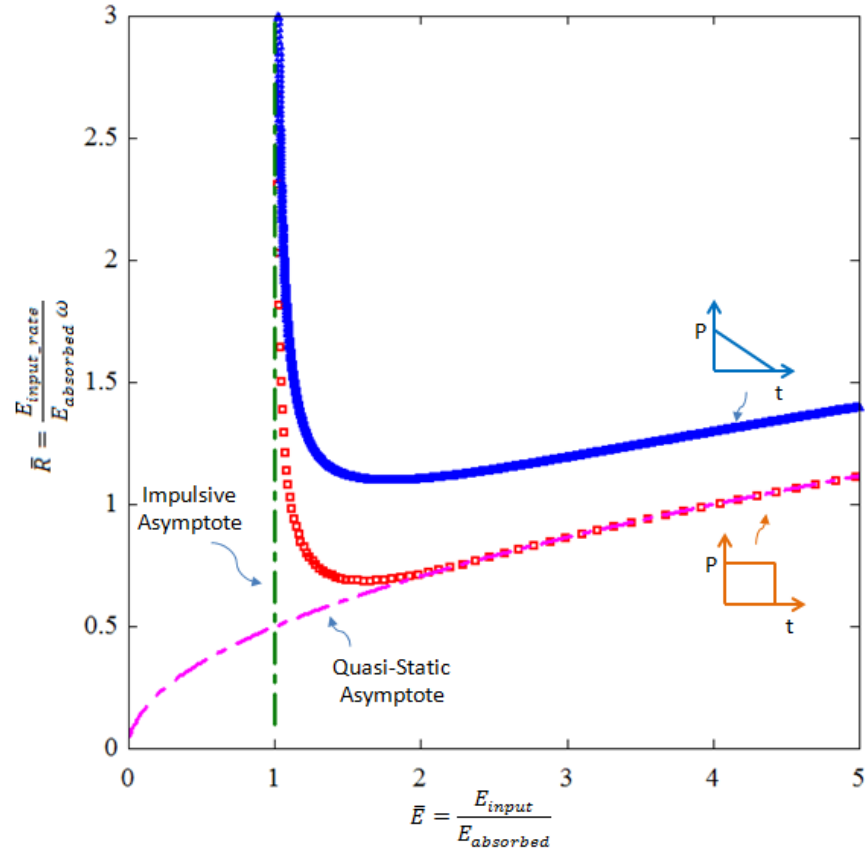


Figure 5. E-R Diagrams for rectangular and triangular loads [3].

The minimum energy required to cause a desired response is equal to the minimum energy input, the energy input value at the impulsive asymptote. For lower input energy rates, more energy is required to be delivered to the system since the energy difference is larger at lower rates. The quasi-static asymptote is no longer a straight line and is defined Equation (15).

$$\bar{R} = \frac{\sqrt{\bar{E}}}{2} \quad (15)$$

RESEARCH TOPICS, METHODOLOGY, AND RESULTS

Validation of P-I to E-R Conversion Equations

A P-I diagram for a beam subjected to a force pulse (as defined by its appropriate β , will be transformed to the E-R diagrams by using Equations (16) and (17) that define the energy input and its rate.

$$E_{input} = \frac{(I_{impulse})^2}{2 \cdot M_{mass}} \quad (16)$$

$$E_{input_{rate}} = \frac{E_{input} * F_o}{I_{impulse}} \quad (17)$$

The results were validated by using the computer code DSAS [9]. Dynamic Structural Analysis Suite (DSAS) is a multifunctional structural analysis program capable of modeling the response of a wide range of structural components under static or dynamic loads. DSAS has been in development since 1979, and many publications demonstrated its capabilities. The current version is written in C# using object-oriented programming principles and supports the latest operating systems and processor technologies. The component library includes reinforced concrete beam, column, and joists, steel beams and columns, CMU and brick masonry walls, reinforced concrete slabs and boxes, wood panels, and simple or advanced mass-damper systems. It can be applied for the analyses of both above ground and underground RC boxes and include ground shock and medium-structure interaction effects. DSAS has fully nonlinear material models and includes geometric nonlinear analyses capabilities. In addition to performing time-history analyses for the various structural elements, DSAS can generate moment-curvature and resistance (load-deflection) functions for the structural components. DSAS has built-in capability to generate pressure-impulse or load-impulse diagrams for any of

the components mentioned above. Since the simulations are performed in only a matter of seconds, the program is well suited for an iterative design procedure.

Figures 6 and 7 show the comparisons of the proposed approach with the analytical solutions and the numerical solutions derived with DSAS for rectangular and triangular load pulses. Figures 6a and 7a show the normalized (i.e., unitless axes) \bar{R} vs. \bar{E} curves, as defined by Equations (10) and (11). Figures 6b and 7b show the actual E-R diagrams for a given beam, where the energy input is measured in kJ and the energy input rate is measured in kW. One notes that the values obtained from the SDOF code DSAS fall along the analytical curves, and that the radius of the numerical points does not represent a data distribution (i.e., the actual data points are at the center of the plotted circles). Also, the SDOF analyses produced hundreds of output points, but only a representative number is shown in the figures for clarity.

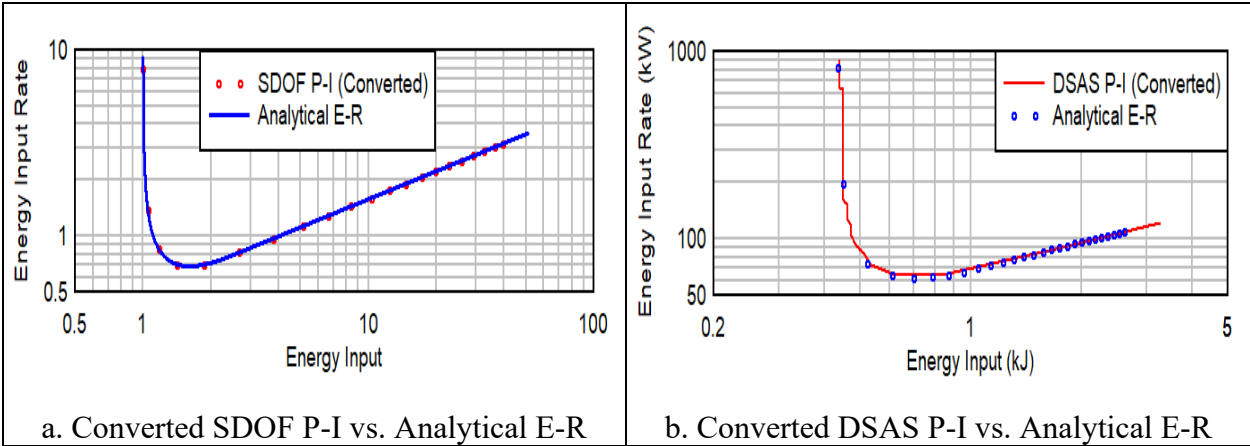


Figure 6. E-R diagram comparisons for rectangular load pulse.

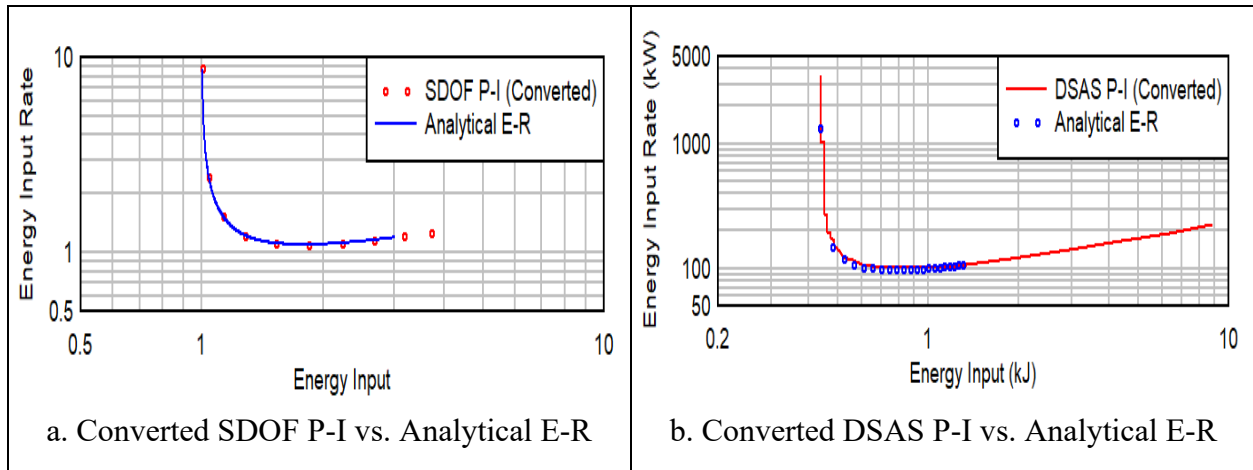


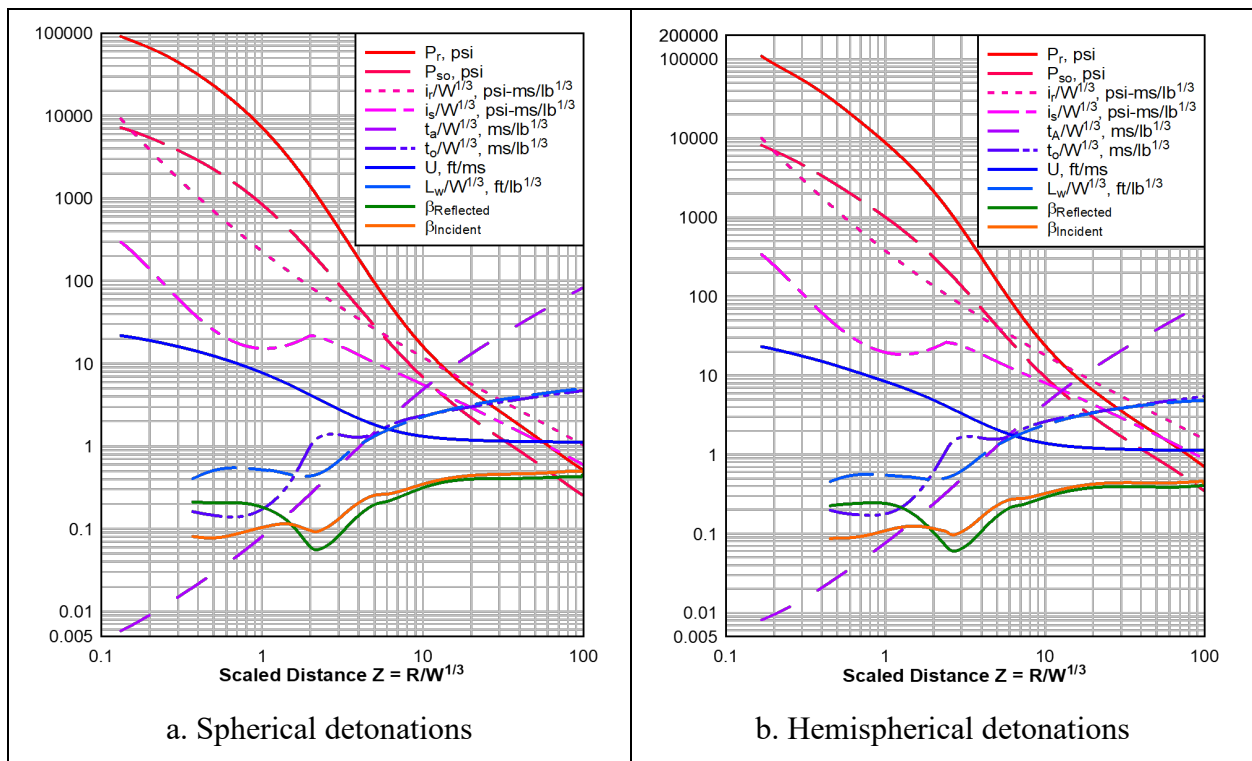
Figure 7. E-R diagram comparisons for triangular load pulse.

Results for Load Pulse Shape Factor (β)

The role of the Load Pulse Shape Factor (β) was presented previously, herein, and the following discussion is aimed at illustrating how one may apply this concept.

Beta in the impulsive domain: The combinations of peak load and impulse that fall within the impulsive domain land directly on the impulsive asymptote, and the calculation of the impulsive asymptote does not depend on the Beta value. Therefore, the shape of the load vs. time plot does not influence values in this range. *Beta in the quasi-static domain:* The combinations of peak load and impulse that fall within the quasi-static domain land directly on the quasi-static asymptote. The calculation of the quasi-static asymptote also does not rely on the Beta value, and the data points in this region are not affected by the Beta value. *Beta in the dynamic domain:* The combinations of peak load and impulse that fall within the dynamic domain do not land on either the impulsive or quasi-static asymptote. These values must be calculated using a numerical procedure in which the shape of the load vs. time plot is significant. Recall that a rectangular load pulse has a $\beta = 1$, and a triangular load pulse has a $\beta = 1/2$. Since each of these values yielded a different curve, it is expected that a load pulse with a Beta value will also produce a

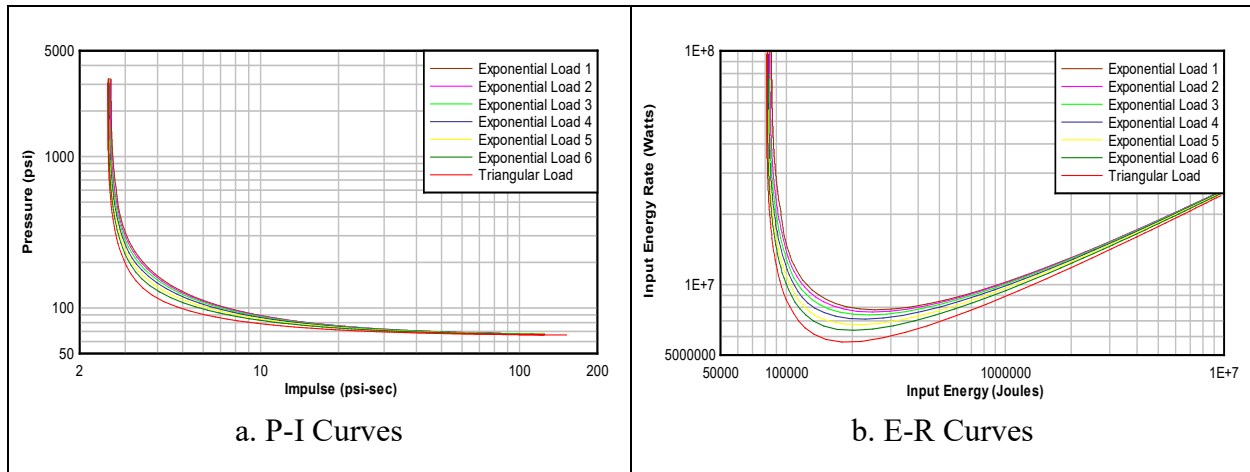
slightly different curve in the dynamic region. The dynamic domain does not have a set limit on the boundaries. While it is easy to determine the boundaries of the impulsive and quasi-static domains, by determining where the asymptotes begin, it is not as easy to set limits on the where the dynamic domain begins and ends. It is easier to define the dynamic domain since the data points do not fall in either of the other two domains. One can use Equation (6) to derive β values for spherical and hemispherical detonations and add them to the corresponding charts from UFC 3-340-02 [10], as shown in Figure 8. It should be noted that Figure 8 was extracted from [10] with the graph software DPlot [11], and the curves for β were inserted into the originals. The units used in [10] are US Standard, and the same units were kept in this study.



1 psi = 0.006895 MPa
 1 lb = 0.4536 kg

Figure 8. Calculated β values for spherical and hemispherical detonations. [10]

The load pulses, as shown in Figure 3 were analyzed with the computer code DSAS [9] to produce the corresponding P-I curves, as shown in Figure 9a. Applying Equations (16) and (17) enables one to convert these P-I curves to E-R curves, as shown in Figure 9b.



1 psi = 0.006895 MPa

Figure 9. P-I and E-R diagrams for different load pulse shapes.

Energy Flow Analysis

It is well known that most of the energy released from an event does not reach a desired target. In the case of a hemispherical detonation, the energy waves propagate away from the detonation site in the form of an expanding hemisphere. It would be useful to designers to be able to determine how much energy will reach the structure and at what rate that energy will do so. If these values could be calculated, a designer could generate an E-R diagram for a desired response of a structure and determine whether the amount of energy released from an event will cause the desired response. One proposed way to determine how much energy will reach the structure is to calculate how much energy is released from the detonation and subtract energy losses, using thermodynamics principles. Another type of energy loss that happens is energy lost to ground shock, which has been shown to be roughly 14% of the total available energy [7]. The largest form of energy loss comes from the fact that the area of the structure that will feel the

energy wave could be small compared to the overall area of the energy hemisphere. By studying the forms in which energy will be “lost,” one could theoretically determine how much energy and at what rate it might reach a specific structure. This approach allows the user to analyze a structural element in the energy domain, by using the E-R diagram to determine if the load from the event could fail the element. The user would not have to determine the pressure and load duration to run a dynamic analysis, but rather could just plot the point corresponding to the energy released from the event over the E-R diagram to check for failure.

This approach is illustrated for a fixed supported reinforced concrete (RC) beam that was 6 inches wide x 12 inches deep x 15 feet long (0.152 m x 0.305 m x 4.572 m) . The concrete compressive strength was 5,000 psi (34.5 MPa) and the yield strength of the steel reinforcement was 69,000 psi (475.7 MPa). The beam was reinforced with (2) #6 bars at the top and bottom of the section. Shear reinforcement was provided with #4 stirrups spaced at 12 inches (0.305 m) on center. The loading was obtained from a TNT charge that was suspended at different heights above the center of the beam. Each loading case is represented by the scaled distance, Z , as defined in Eq. (5), and the blast load characteristics were extracted from Figure 8a (i.e., spherical explosions). The pressure distribution on the top surface of the beam was calculated with the ‘Loads on Structures’ option in computer code ConWep [12]. That enables one to select a triangular equivalent uniformly distributed pressure vs. time that represents the actual nonuniform pressure distribution under such conditions. The RC beam was analyzed with the computer code DSAS [9] that provides the dynamic responses in the time and P-I domains. Then, the P-I values were transformed to E-R values by Equations (16) and (17). In this example, four energy deposition cases (i.e., energy magnitude and its flow rate for the corresponding scaled distances) are shown in Table 4.

Table 4. Equivalent triangular load from energy depositions.

Deposition Number	Scaled Distance ft/lb ^{1/3}	Energy Input (kJ)	Energy Input Rate (kW)	Impulse (psi*sec)	Pressure (psi)	Duration (msec)	DSAS Result
1	1.6	59.6	262771	1.332	5876	0.453	No Failure
2	1.4	73.9	314608	1.484	6314	0.470	No Failure
3	1.2	89.6	368977	1.634	6726	0.486	Failure
4	1.0	115.6	455101	1.855	7306	0.508	Failure

1 psi = 0.006895 MPa

1 lb = 0.4536 kg

1 ft = 0.305 m

Plotting these energy deposition cases on the E-R diagram for the beam in Figure 10 show which points could cause the flexural failure. One notes from Figure 10 that energy depositions 1 and 2 would not cause failure, while energy depositions 3 and 4 would cause the failure. Once the E-R diagram is created, dynamic analyses are not needed to determine the level of structural response. Connecting the load points creates a load path curve in E-R units whose intersections with E-R diagrams defines failure conditions, as shown in Figure 10. Only the amount of input energy and input energy rate that reach the structural element from an energy releasing event need to be known to analyze the structure.

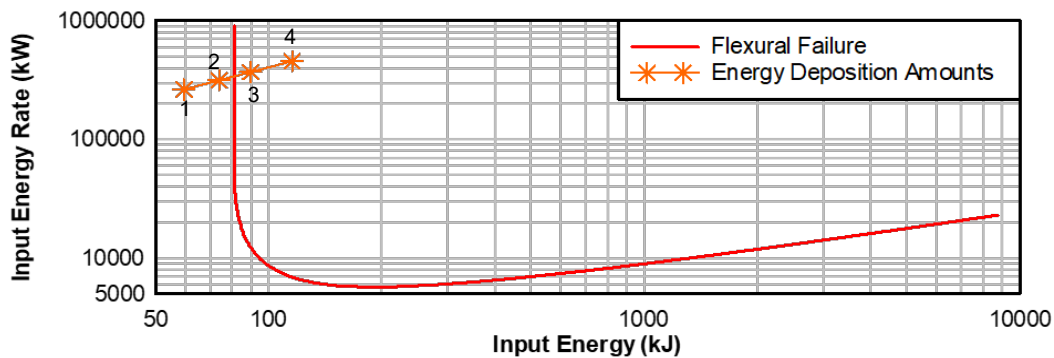


Figure 10. E-R diagram with overlaid energy deposition curve.

CONCLUSIONS

This study was aimed at validating the conversion equations from P-I data to E-R data and applying the methodology to more realistic scenarios. The conversion equations were successfully validated by comparing multiple cases using converted P-I data from DSAS and the analytical based energy solutions. Another focus in this research was to determine the role that the load pulse shape factor β in the calculation of P-I and E-R diagrams. It was found that different β values yielded slightly different P-I and E-R diagram throughout the dynamic region. However, the asymptotes for all the cases still converged to the same value, regardless of the β value, showing that β only plays a significant role in the dynamic domain region. This is an interesting finding that, if the loading is mostly impulsive, enables the user to apply simple load pulses to determine P-I or E-R diagrams. The simplified load pulses allow for a more efficient process in creating the diagrams, and their use can be justified if the region near the asymptotes are of more interest due to the given loadings. The final aspect of this research was to examine more realistic scenarios using the E-R diagram approach. This was done by creating an E-R diagram for a flexural failure of a beam. A series of “load points,” or energy depositions, were plotted on the same graph as the E-R diagram. The four energy depositions were transformed to pressure vs. time plots using the P-I to E-R conversions equations. These loads were checked with the computer code DSAS to ensure the expected results from the E-R diagram. Each of the four points caused the beam to react, as expected. Two of the load points (i.e., energy depositions) did not cause a failure, while the other two loads caused failure. This confirmed that the approach is valid and can be used to analyze a structural element, based on energy flow conditions.

ACKNOWLEDGEMENT

The authors wish to acknowledge the generous support from AFRL/RW for this study.

REFERENCES

1. Willems, K., and Krauthammer, T., “An Energy Flow Based Approach to Structural Response Assessment,” Final Technical Report on Contract FA8651-15-D-0310 Task 1, to Air Force Research Laboratory (AFRL/RWML), CIPPS-TR-002-2018, Center for Infrastructure Protection and Physical Security, University of Florida, Limited Distribution under Statement D, August 2018.
2. Biggs, J. M., *Introduction to Structural Dynamics*, New York, NY, McGraw-Hill Book Company, 1964.
3. Tsai, Y.K., and Krauthammer, T., “Energy Based Load-Impulse Diagram for Structural Elements,” Technical Report CIPPS–TR-002-2015, Center for Infrastructure Protection and Physical Security, University of Florida, April 2015.
4. Tsai, Y.K., and Krauthammer, T., *Energy Based Load-Impulse Diagrams*, Engineering Structures, Vol. 149, pp. 64-77, October 2017.
5. Tsai, Y.K., and Krauthammer, T., *Energy Based Load-Impulse Diagrams with Multiple Failure Modes for Blast-Loaded Reinforced Concrete Structural Elements*, Engineering Failure Analysis, Vol. 104, pp. 830-843, 2019.
6. Baker, W.E., Cox, P.A., Westine, P.S. , Kulesz, J.J., and Strehlow, R.A., *Explosion hazards and evaluation*, Amsterdam, NY, Elsevier Scientific Pub Co, 1983.
7. Krauthammer, T., *Modern Protective Structures*, CRC Press, Taylor and Francis Group, 2008.

8. Krauthammer, T., Astarlioglu, S., Blasko, J., Soh, T.B., and Ng, P.H., *Pressure-Impulse Diagrams for the Behavior Assessment of Structural Components*, *International Journal of Impact Engineering*, pp. 35:771-83, 2008.
9. Astarlioglu, S., and Krauthammer, T., “Dynamic Structural Analysis Suite (DSAS),” User Manual, Version 4.0, Technical Report CIPPS–TR-002-2012, Center for Infrastructure Protection and Physical Security, University of Florida, March 2012.
10. DOD, “Structures to Resist the Effects of Accidental Explosions,” Unified Facilities Criteria (UFC), UFC 3-340-02, 5 September 2008, Change 2, 1 September 2014.
11. DPlot, <https://www.dplot.com/index.htm>
12. Hyde, D.W., User Guide for Microcomputer Program ConWep, Application of TM 5-855-1, “Fundamentals of Protective Design for Conventional Weapons”, Instruction Report SL-88-1, Department of the Army, Waterways Experiment Station, Corps of Engineers, April 1988 (Revised 22 February 1993).